



UNIVERSITY OF READING  
Department of Mathematics  
Numerical prediction of flood plains using a  
Lagrangian approach

Jean-Francois VUILLAUME

October 29, 2012

**Declaration** A dissertation submitted in partial fulfilment of the requirement for the degree of "Mathematics and Numerical Modelling of Atmosphere and Ocean"

" I confirm that this is my own work, and the use of all material from other sources has been properly and fully acknowledged."

Reading, United Kingdom, October 29, 2012

**Acknowledgements** I would like to acknowledge Prof. Mike Baines for supervising this project and expanding the subject with flourishing numerical ideas.

Thanks to:

Nicholas Bird, Dr Anne Verhoef and Dr. Bruce Main for discussions;

Industri Energi (IE), industry worker union in Norway to provide me with a study grant to finance partially the study

Jenjira, Tar and Laszlo for sharing their warm friendship

The Chaplaincy and the peer support project of the University of Reading

The Cold ash Retreat centre

El Grupo De Capoeira Sao Jose Dos Carpinteiros

Jean-Francois October 29, 2012

**Dedication** I would like to dedicate this thesis to my family ...

## **Abstract**

Flood events have large consequences on human society in terms of impact on human life and economy. In the current climate change situation, increase of heavy rain will contribute to an increase of flood events both in intensity and frequency. Groundwater flood is a particular flood event which involves the rising of the groundwater table to the surface due to previous infiltration. Numerical modelling codes based on physical laws describing the velocity and water column change are powerful tools for flood simulating extensions and intensity forecasts. We have developed a coupled code consisting of a one dimensional shallow water equation approximation together with a thin film equation to describe the behaviour of the groundwater flood. A Lagrangian description is used throughout because it is particularly adapted to the problem of both the shallow water and thin film equations. In addition, high order numerical resolution of high order equation is sought using an adaptive moving mesh to improve the accuracy of the solution. The model proposed leads to a finite difference numerical draft model of the groundwater flood in 1D for single sources. It will needs further testing to improve its stability and flow continuity. Further development of the code may imply a 2D development, a finite element version of the code more suitable to solve the flow computation on a complex surface, consideration for roughness and the use of implicit method.

# Contents

<b>1</b>	<b>Introduction</b>	<b>7</b>
<b>2</b>	<b>A moving mesh : A velocity-based moving mesh method</b>	<b>13</b>
2.1	Finite Difference Methods . . . . .	14
2.2	Mass conservation . . . . .	14
2.3	Local mass conservation . . . . .	14
2.4	Moving mesh . . . . .	15
<b>3</b>	<b>One-dimensional shallow water equation approximation: The Saint-Venant approximation</b>	<b>16</b>
3.1	Eulerian description of fluid . . . . .	17
3.1.1	Mathematics equations . . . . .	17
3.1.2	Finite difference discretization . . . . .	17
3.1.3	Volume control . . . . .	18
3.2	Semi-Lagrangian description of fluid movement or trajectory-based method . . . . .	22
3.2.1	Mathematical equations . . . . .	22
3.2.2	Finite difference discretization . . . . .	22
3.2.3	Boundaries conditions . . . . .	23
3.3	Fully Lagrangian fluid dynamic description: The Verlet scheme	23
3.3.1	Mathematical formulation . . . . .	26
3.4	Global and local mass conservation . . . . .	26
3.4.1	Discretization and algorithm implementation . . . . .	27
3.4.2	Numerical Results of Saint-Venant equations using the Verlet scheme . . . . .	27
<b>4</b>	<b>Non linear diffusion: Thin film equation</b>	<b>35</b>
4.1	Mathematical formulation . . . . .	35

4.2	Finite Difference discretization . . . . .	36
4.3	Boundary conditions . . . . .	37
4.3.1	Left boundary, velocity of nodal point 0 . . . . .	37
4.3.2	Right boundary, velocity of nodal point N: Thin film precursor . . . . .	37
4.4	Numerical Results of the thin film equation . . . . .	38
<b>5</b>	<b>Coupling model for flood modelling</b>	<b>41</b>
5.1	Mathematical formulation . . . . .	41
5.2	Global and local mass conservation . . . . .	43
5.3	Numerical modelling results . . . . .	44
<b>6</b>	<b>Conclusions and Further Work</b>	<b>47</b>
6.1	Conclusions . . . . .	47
6.2	Results . . . . .	48
6.3	Further Work . . . . .	49

# List of Figures

1.1	Flooding facts in the UK . . . . .	8
1.2	Example of flooding risk map (From Ordnance Survey Ireland, All rights reserved. Licence number 2010/15CCMA/Galway County Council) . . . . .	10
1.3	Schematic model of the numerical problem ( <i>From Baines et al., 2012, Unpublished</i> ) . . . . .	11
3.1	Figure for control volume approach to discretization of continuity equation [1] . . . . .	19
3.2	1D Saint-Venant flow at $t = 100$ s (Computation FORTRAN, visualization MATLAB) . . . . .	20
3.3	1D Saint-Venant flow at $t = 200$ s (Computation FORTRAN, visualization MATLAB) . . . . .	21
3.4	1D Saint-Venant flow at $t = 10$ s (Computation FORTRAN, visualization MATLAB) . . . . .	24
3.5	1D Saint-Venant flow at $t = 70$ s (Computation FORTRAN, visualization MATLAB) . . . . .	25
3.6	Results of the computation of the Saint-Venant equations using the Verlet scheme, $N = 51$ nodes and initial condition $h^0 = a \times \left(1 - \left(\frac{x^2}{4}\right)^2\right)$ (Computation and visualization tool MATLAB). . . . .	28
3.7	Results of the computation of the Saint-Venant equations using the Verlet scheme, $N = 11$ nodes and initial condition $h^0 = a \times (1 - \tanh(x))$ (Computation and visualization tool MATLAB). . . . .	29

3.8	General results of the computation of the Saint-Venant equations using the Verlet scheme, $N = 101$ nodes and initial condition $h^0 = 1$ for $x = [0, 50]$ and $h^0 = \left(1 - \left(\frac{x^2}{4}\right)^2\right)$ for $x = [50, 100]$ , $dt = 0.00001s$ , $dx = 1m$ (Computation and visualization tool MATLAB). . . . .	31
3.9	Front zoom results of the Saint-Venant equations computation using the Verlet scheme, $N = 101$ nodes and initial condition $h^0 = 1$ for $x = [0, 50]$ and $h^0 = \left(1 - \left(\frac{x^2}{4}\right)^2\right)$ for $x = [50, 100]$ , $dt = 0.00001s$ , $dx = 1m$ . Zoom on the front wave (Computation and visualization tool MATLAB). . . . .	32
3.10	Left boundary results of the Saint-Venant equations computation using the Verlet scheme, $N = 101$ nodes and initial condition $h^0 = 1$ for $x = [0, 50]$ and $h^0 = \left(1 - \left(\frac{x^2}{4}\right)^2\right)$ for $x = [50, 100]$ , $dt = 0.00001s$ , $dx = 1m$ . Zoom on the Left boundary (Computation and visualization tool MATLAB). . .	33
3.11	Oscillations on the water front associated with the Saint-Venant equations computation using the Verlet scheme, $N = 101$ nodes and initial condition $h^0 = 1$ for $x = [0, 50]$ and $h^0 = \left(1 - \left(\frac{x^2}{4}\right)^2\right)$ for $x = [50, 100]$ , $dt = 0.00001s$ , $dx = 1m$ . Zoom on the Left boundary (Computation and visualization tool MATLAB). . . . .	34
4.1	Results of the computation of the thin film equation for $N = 11$ nodes.(Computation and visualization tool MATLAB) . . .	39
4.2	Illustration of the main features of the thin film script (Computation and visualization tool MATLAB). . . . .	40
5.1	Schematic illustration of the coupled flow problem . . . . .	42
5.2	Numerical result of the coupled model at time $t = 0$ s, $t = 20$ s and $t = 40$ s . . . . .	44
5.3	Numerical result of the coupled model at time $t = 0$ s, $t = 20$ s, $t = 40$ s, $t = 60$ s, $t = 80$ s, $t = 100$ s . . . . .	45

# List of Tables

**Definition** *Groundwater* : Aquifer which is located underground. In this case the aquifer is unconfined and pressure increase results in the rise of the water column

*Open channel flow* : Flow of water in a channel in which the top part contains a free boundary

*Groundwater flood* : Flood due to the rise of the groundwater at the surface

*Flash flood* : Flood due to quick heavy rain. Infiltration that exceeds the threshold of the maximum soil infiltration is called run-off flow, which can create hill-slope flood flow

*Verlet* is a Physicist pioneered the computation of molecular dynamics models simulation. It refers to a particular scheme called "Verlet scheme"

**Nomenclature**  $h$  : The height of the water column (in metres m)

$x$  : Position in the x direction (in meters m)

$u$  : Velocity of the water in the x direction (in metres per seconds  $m.s^{-1}$ )

$t$  : Time (in seconds s)

$g$  : Gravity constant,  $g = 9.80665$  (in  $m.s^{-2}$ )

*slope* : Slope of the bottom

*Manning* : Coefficient of roughness

# Chapter 1

## Introduction

Flooding research constitutes an important research topic driven by its major impact on society. The damage due to flood is costly and insurance costs to prevent flood damage are high. Worldwide, coastal, riverine and flash floods are responsible for more than 50% of fatalities and for about 30% of the economic losses caused by all natural disasters.

In the United Kingdom, property, land and assets to the value of £214 billion are at risk of flooding in England and Wales. The Environment Agency spends £300 millions a year on flood defences, 43% of existing flood defences being in a fair, poor or very poor state of repair. The damage bill from the devastating floods of 2007 was in excess of £3 billion. A map of England exposure risk to groundwater flood was published by the Environment Agency (Figure 1.1)

These natural hazards have a certain degree of predictability and the keys to minimize the damage are in the precision of the flood extent and intensity prediction. Different flood events such as heavy rain, tsunamis, over banking in channels and groundwater occur. Accurate determination of height and extension of the flood require numerical modelling tools based on discretization of physical laws. In this study, flood issue from a groundwater rise to the surface is modelled by finite differences, in a Lagrangian reference frame and in one dimension. Soil, rock properties, topography and rain intensity play a strong role in this process but those phenomena are not modelled in this project.

**Around 5 million people live in flood risk areas in England and Wales.**

(source: Environment agency.)

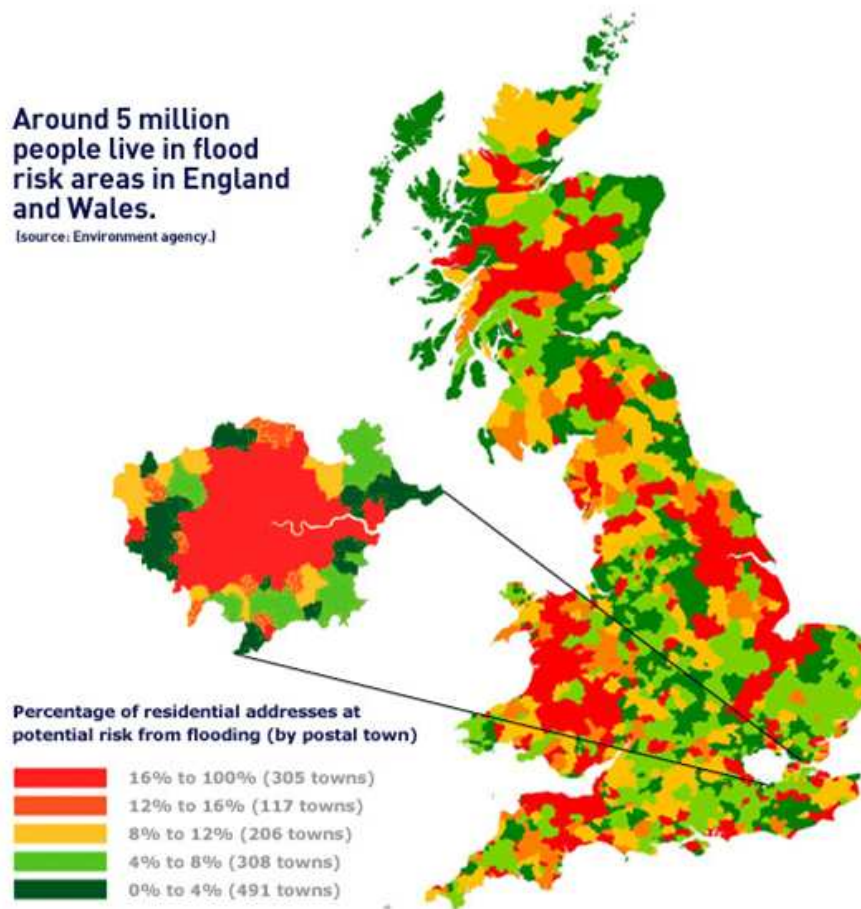


Figure 1.1: Flooding facts in the UK

During this study, only the groundwater flood process after reaching the surface was studied. To model this effect, a one dimensional depth averaged approximation of the Navier-Stokes was used called the Saint-Venant equations.

The Navier-Stokes equations describe the motion of fluid and arise from applying Newton's second law to fluid motion. The Shallow Water Equations (SWEs) are a vertically averaged approximation of the Navier-Stokes equation. The vertical averaging is determined using the boundary conditions and by averaging the velocity over the depth. This dissertation describes the derivation steps of the averaged depth Shallow water equation and the associated approximations. The depth averaged method is a standard current technique to approximate the Navier-Stokes equations to shallow water approximation. The one dimensional approximation of the Shallow water equations are the Saint-Venant equations or open channel flow equations (Olsen, 2012 [1]).

The latest numerical scheme and strategies to optimize flood depth averaged free surface problem have been compiled by Delis et al., 2010 [2]. Furthermore, detail of the derivation of the approximation of the Shallow water equations currently used are developed by Dawson and Mirabito, 2008, [3]. Commercial numerical codes developed since the '60's, include MIKE from Danish Hydrological Institute (DHI), HEC-RAS from the American Hydraulic Engineering Centre, TUFLOW. Recent open source code are now available for flood modelling purpose such as OPEN OpenCFD [4]. Those models are used for channel, overbank flood or heavier rain flood. At present, no model is specifically dedicated to groundwater flooding but there is a growing interest related to the groundwater issue.

Output of numerical model are used to produced flooding risk maps as illustrated Figure 1.2 The Saint-Venant equations are coupled to a thin film equation to model the diffusion of the water with low water fluxes.

The thin film equation is a non-linear 4th order equation which describes the spreading of a fluid on a surface. The two equations, Saint-Venant for linear uniform flow, and diffusion, are coupled to describe more precisely a groundwater flood process.

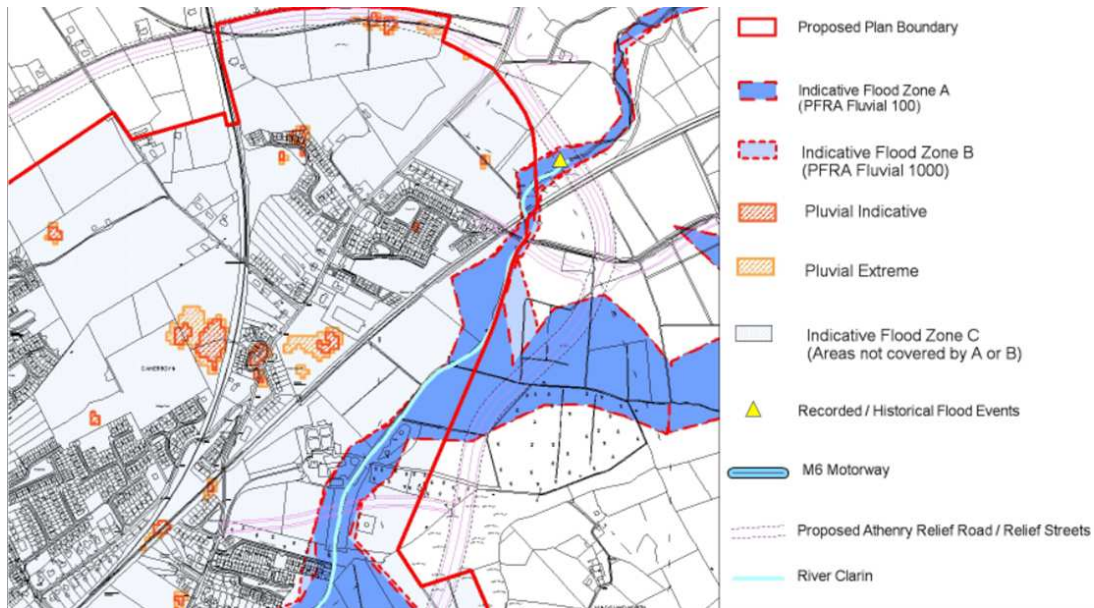


Figure 1.2: Example of flooding risk map (From Ordnance Survey Ireland, All rights reserved. Licence number 2010/15CCMA/Galway County Council)

A recent research project called FUSE (Floodplain Underground SENSors) [5] uses a high-density, wireless, underground Sensor Network to quantify floodplain hydro-ecological interactions. It investigates the Field groundwater table change with flood consequence. It allows monitoring of the groundwater level by geophysics, i.e. electromagnetic methods, with a high resolution. In the long term the project will improve our understanding of groundwater flood forecast and could possibly be used as an early alert tool for groundwater floods.

Numerical modelling software is a key tool to address the degree of predictability of a flood event: Numerical modelling improvements will minimize the damage by improving the precision of flood front location and the height of the water wave. The present project also makes use of a Lagrangian frame of reference, resulting in interesting and challenging numerical modelling issues with maximum time steps in coupling the systems of equations: Saint-Venant for laminar flow and thin film for non-linear diffusion, using a moving mesh strategy based on velocities.

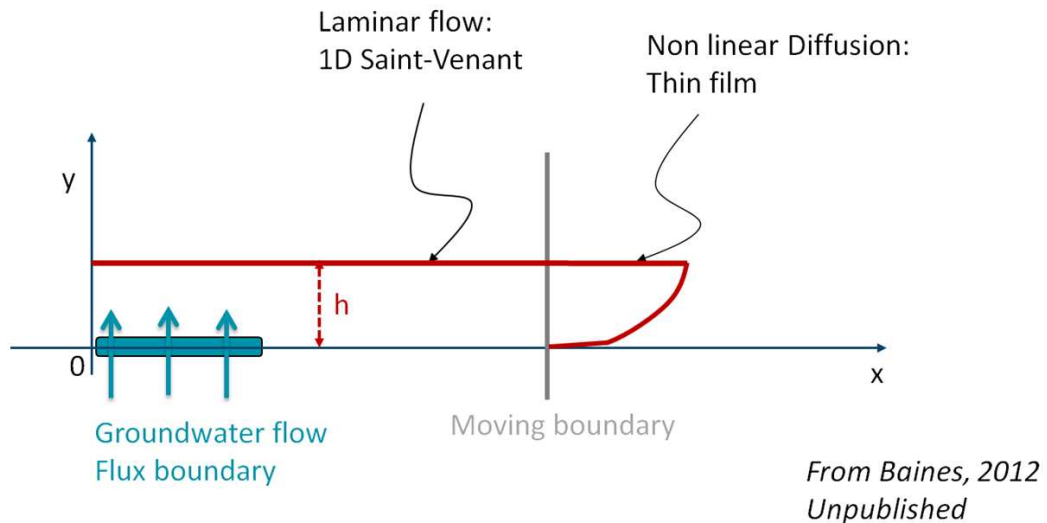


Figure 1.3: Schematic model of the numerical problem (*From Baines et al., 2012, Unpublished*)

The thin film equation is a diffusion problem described by a 4th non linear differential order equation. It describes the spreading of a thin film on a surface. Several publications are related to this problem which have several industrial applications (O'Brien and Schwartz, 2002 [6]). In our case, problem of capillary and inter-facial tension is neglected due to the dynamic of the fluid.

The coupling of the two problems is a based on theoretical assumptions which haven't been developed and published yet. Hence, the use of this idea will be submitted to criticism based on this first project. The problem covered by this work is illustrate by the Figure 1.3 where the two flow domains are illustrated. The location of the groundwater source flow at the left boundary and the moving free boundary at the right hand of the model are illustrated as well.

**Summary** The first chapter introduces the objectives of the project and the limitations of the model and discusses recent advances in flood numerical modelling. Chapter 2 reviews the moving mesh method and the velocity moving mesh method used for this problem. Chapter 3 describes the Saint-Venant equations, 1D approximation of the shallow water equations (also called the open channel flow equations). Mathematical and numerical scheme development is described including the Lagrangian frame of reference. Chapter 4 describes a version of the 4th order non linear diffusion equation called the thin film equation and its modelling using a moving mesh strategy. Chapter 5 describes the coupling strategy used to coupled the two type of equations and resolve moving boundaries. Finally, Chapter 6 concludes and gives further work perspectives.

## Chapter 2

# A moving mesh : A velocity-based moving mesh method

This chapter describes a method based on a moving mesh strategy. This method uses a velocity based moving mesh method, particularly well-adapted for Lagrangian fluid movement. Moving meshes or dynamic meshes are a numerical modelling strategy to minimize the number of grid points used for a dynamic problem compared to a static grid while preserving the physics of phenomena. The method chosen is based on local mass conservation for each discretized element (Baines et al., 2011 [7]), which is consistent global mass conservation. The method allows the configuration of the velocity of the mesh for each nodal point of the mesh (Bhattacharya, MSc 2004 [8]). The local conservation is assured for each time step. The velocity is obtained by differentiating the mass conservation equation. The new mesh locations are obtained from the nodal velocities by a time step method. The method is particularly adapted to surface flow problems. Several moving meshes methods has been developed and this area of research is ongoing (Budd et al., 2009 [9]), having strong potential in climate models for example (Weller et al, 2009 [10]).

## 2.1 Finite Difference Methods

The Finite Difference Method (FDM) is used in this project. Finite Element Method was used by Bhattacharya. B., 2004 [8] and Baines et al., 2005 [11] with successful results. The coupled method consists of discretizing the domain with  $N$  nodes and computing the Partial Differential Equations of Saint-Venant and the thin film method over time using traditional time steps. Both sets of equations became discretized by an explicit method.

## 2.2 Mass conservation

We considered the non linear thin film equation

$$\frac{\partial h}{\partial t} = \frac{\partial}{\partial x} \left( h^3 \frac{\partial^3 h}{\partial x^3} \right) \quad (2.1)$$

over the domain  $x = [-1, 1]$  with  $h = 0$  at the free boundaries ( $x_0(t)$  and  $x_N(t)$ ). We can identify two steps in the velocity based moving mesh. First, the velocity of each nodal point is computed. Previous work has included the development of a moving mesh method for a self similar problem, Bird., 2012 [14]. The typical equation used was :

$$\frac{\partial h}{\partial t} = \frac{\partial}{\partial x} \left( h \frac{\partial^3 h}{\partial x^3} \right) \quad (2.2)$$

with  $h = 0$  at free boundaries.

Secondly, the local mass conservation law is used to determine the new height of the water column. Global mass conservation is assured by the boundary conditions.

## 2.3 Local mass conservation

The local mass conservation between discretized points is assumed over time. It is defined as

$$\int_{x_{i-1}(t)}^{x_{i+1}(t)} h(x, t) dx = \rho_i \quad (2.3)$$

where  $\rho_i$  represent the local mass at the node  $i$  which remains constant for all time. A discrete midpoint approximation of the integral (Equation 2.3)

gives:

$$(x_{i+1} - x_{i-1})h_i = \rho_i \quad (2.4)$$

for

$$i = 2, \dots, N - 1$$

Next, the new location of the node is computed and height of the water column is recomputed based on equation 2.3 for each  $h_i$

## 2.4 Moving mesh

Knowing the velocity of the node at each node, the new location of the nodes  $x_i^{n+1}$  can be calculated from the previous node location  $x_i^n$  by the expression:

$$x_i^{n+1} = x_i^n + v_i \times dt \quad (2.5)$$

where  $v_i$  represent the velocity of each node and  $dt$  the time step used. Care have to be taken for the chose of  $dt$ , high value of the time step could conduct to node overlapping since the node velocity are different. In the other hand, low  $dt$  value will conduct to slow the computation code.

## Chapter 3

# One-dimensional shallow water equation approximation: The Saint-Venant approximation

The Saint-Venant equation describes a one-dimension (1D) approximate shallow water flow used currently for open channel flow. It can be used for a one dimension water flow problem as a simplification of a two-dimension (2D) problem in a 1D context. The equations which described the flow process are derived from the mass conservation and momentum conservation.

Eulerian and Lagrangian descriptions of fluid constitute two ways to describe fluid movement (Price (2006 [12])). The Eulerian approach supposes a fixed reference and the Lagrangian approach a coordinate system moving with the fluid particles. Due to the nature of flooding, the Lagrangian description is particularly adapted to the problem: the equations become simpler and their numerical approximation more precise. Due to the central difference explicit scheme used, a volume corrector is used to compute the height of the water column. The channel is considered with a small slope of 0.006 degree. We begin by considering the Eulerian SWEs, following by a semi-implicit Lagrangian formulation and finally fully Lagrangian. The Verlet scheme is used for the Lagrangian SWEs.

## 3.1 Eulerian description of fluid

There are several schemes available to solve the Saint-Venant equations. For the Eulerian approach, we used space central difference method corrected by a predictor corrector as illustrated by Olsen., 2012 [1].

### 3.1.1 Mathematics equations

We define the variables:

$h$ : The height of the water column, a function of  $x$  and  $t$

$x$ : Position in the x direction

$u$ : Velocity of the water in the x direction, also a function of  $x$  and  $t$

We assume the following equations of continuity and momentum conservation:

Continuity equation:

$$\frac{\partial h}{\partial t} + \frac{\partial(uh)}{\partial x} = 0 \quad (3.1)$$

Momentum equation:

$$\frac{\partial u}{\partial t} + u \frac{\partial u}{\partial x} + g \frac{\partial h}{\partial x} = 0 \quad (3.2)$$

### 3.1.2 Finite difference discretization

We discretize both equations by a simple finite difference method, the Forward-Time Central-Space (FTCS) scheme. Both explicit and a semi-implicit schemes were used. The simplicity of the formulation makes the algorithm attractive even of strong instability. According to Olsen [1], a volume corrector has to be applied due to the high instability of the central difference scheme. The numerical approximations are

$$\frac{\partial h}{\partial t} \approx \frac{h_i^{n+1} - h_i^n}{dt}$$

and

$$\frac{\partial u}{\partial x} \approx \frac{u_{i+1}^n - u_{i-1}^n}{2\Delta x}$$

where  $h_j^n$  is the height of the water column at node  $j$  and at time  $t_n$  of the domain  $x = [0, 1000]$ . Also,

$$\frac{\partial(uh)}{\partial x} \approx u_i^n \frac{h_{i+1}^n - h_{i-1}^n}{2\Delta x} + h_i^n \frac{u_{i+1}^n - u_i^{n-1}}{2\Delta x}, \quad (3.3)$$

leading to :

$$\frac{h_i^{n+1} - h_i^n}{\Delta t} + u_i^n \frac{h_{i+1}^n - h_i^n}{2\Delta x} + h_i^n \frac{u_{i+1}^n - u_i^n}{2\Delta x} = 0 \quad (3.4)$$

Hence,

$$h_i^{n+1} = h_i^n - \frac{\Delta t}{2\Delta x} (u_i^n (h_{i+1}^n - h_i^n) + h_i^n (u_{i+1}^n - u_i^n)) \quad (3.5)$$

where  $dx$  is the spacial increment and  $dt$  the temporal increment. For the equation the explicit form is given by: Which lead to:

$$\begin{aligned} \frac{u_i^{n+1} - u_i^n}{\Delta t} &= u_i^n \frac{u_{i+1}^n - u_i^n}{\Delta x} + g \frac{h_{i+1}^n - h_i^n}{\Delta x} \\ u_i^{n+1} &= u_i^n - \frac{\Delta t}{\Delta x} (u_i^n (u_{i+1}^n - u_i^n) + g(h_{i+1}^n - h_i^n)) \end{aligned} \quad (3.6)$$

The semi-implicit form is defined by:

$$u_i^{n+1} = u_i^n - \frac{\Delta t}{\Delta x} (u_i^n (u_{i+1}^n - u_i^n) + g(h_{i+1}^{n+1} - h_i^{n+1})) \quad (3.7)$$

The Semi-implicit form was used because it considered as more accurate at the time the value of the velocity  $u$  is computed.

### 3.1.3 Volume control

Due to the high instability of the explicit scheme, an implicit volume corrector has to be applied to recalculate the correct velocity and height of the solution. According to Olsen [1], this operator can be defined as: ]

$$h_i^{n+1} = 0.25 \times (u_i^n + u_i^{n+1}) + h_i^n \times \frac{\frac{\Delta x}{\Delta t} - 0.5 \times u}{\frac{\Delta x}{\Delta t} + 0.5 \times u} \quad (3.8)$$

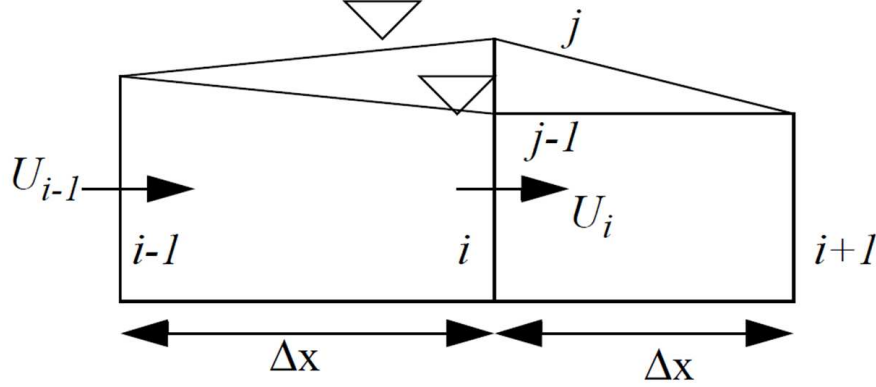


Figure 3.1: Figure for control volume approach to discretization of continuity equation [1]

where  $u$  is defined as:

$$u = \frac{u_i^n + u_i^{n+1}}{2}$$

An illustration of the of the approach related to the Equation 3.8 is illustrated Figure 3.1.  $i - 1, i, i + 1$  represent three cross sections,  $j - 1, j$  two surfaces water. The purpose of the algorithm is to compute the height of the water column at  $j$ . The volume control is based on the computation of fluxes in and out of the volume upstream of  $i$ . The difference between the inflow and the outflow is equal to the volume of water between the two surface at time  $j - 1$  and  $j$  respectively.

The results of the Saint-Venant numerical model are illustrated in Figure 3.2, Figure 3.3 at time  $t = 1$  s,  $t = 20$  s,  $t = 50$  s,  $t = 100$  s,  $t = 150$  s,  $t = 200$  s respectively. The space step is set to  $dx = 1m$  with  $N = 101$  nodal points, the time step was set to  $dt = 1s$ . The Figures shows the propagation of a channel water wave over time. The curve indicates the height and the location of the water level. The front height is well captured. Oscillation at the left boundary can be observed due to the sharp flow change from the discontinuity of the initial condition.

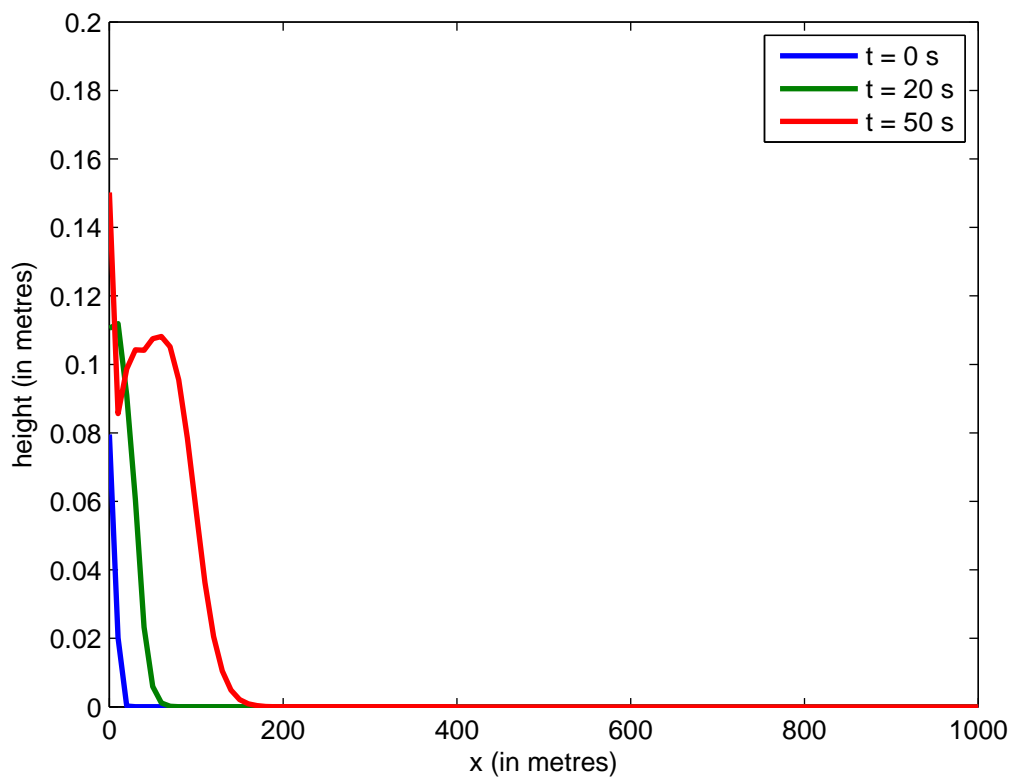


Figure 3.2: 1D Saint-Venant flow at  $t = 100$  s (Computation FORTRAN, visualization MATLAB)

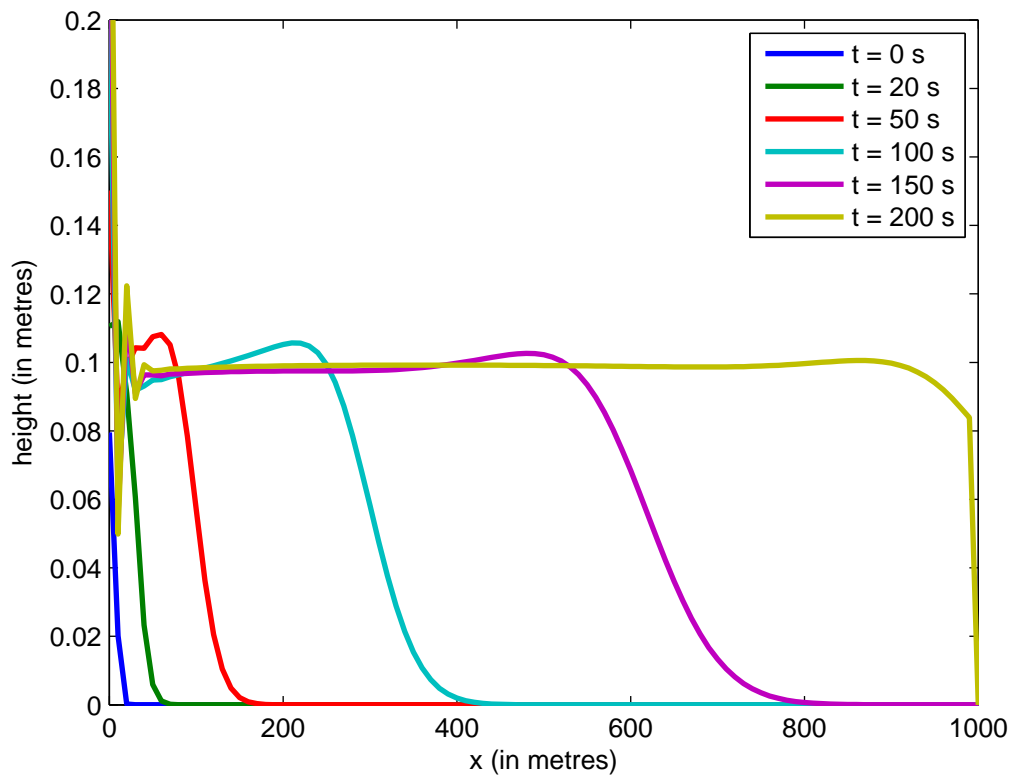


Figure 3.3: 1D Saint-Venant flow at  $t = 200$  s (Computation FORTRAN, visualization MATLAB)

## 3.2 Semi-Lagrangian description of fluid movement or trajectory-based method

The Semi-Lagrangian description of fluid flow is used to simplify the problem. For the Saint-Venant approximation, two steps are needed for the method. First, the height of the water column has to be computed based on the velocity by the continuity equation. In the next step, the new velocity is determined by the momentum conservation equation. We used the definition of Lagrangian fluid movement:

$$\frac{Dh}{Dt} = \frac{\partial h}{\partial t} + u \frac{\partial h}{\partial x} \quad (3.9)$$

### 3.2.1 Mathematical equations

We have the following equations:

Continuity equation:

$$\frac{\partial h}{\partial t} + \frac{\partial(uh)}{\partial x} = 0 \Leftrightarrow \frac{Dh}{Dt} + h \frac{\partial u}{\partial x} = 0 \quad (3.10)$$

Momentum equation:

$$\frac{\partial u}{\partial t} + u \frac{\partial u}{\partial x} + g \frac{\partial h}{\partial x} = 0 \Leftrightarrow \frac{Du}{Dt} + g \frac{\partial h}{\partial x} = 0 \quad (3.11)$$

### 3.2.2 Finite difference discretization

We express the previous equation using a Lagrangian derivative, expressing the new height, new velocity and new position of the water wave: Continuity equation:

$$\begin{aligned} & \frac{Dh}{Dt} + h \frac{\partial u}{\partial x} = 0 \\ \Leftrightarrow & \frac{h_i^{n+1} - h_i^n}{\Delta t} + h_i^n \frac{u_{i+1}^n - u_{i-1}^n}{2\Delta x} = 0 \end{aligned}$$

$$\Leftrightarrow \frac{h_i^{n+1} - h_\alpha^n}{\Delta t} = -h_i^n \frac{u_{i+1}^n - u_{i-1}^n}{2\Delta x}$$

$$\Leftrightarrow h_i^{n+1} = h_\alpha^n - h_i^n \times (u_{i+1}^n - u_{i-1}^n) \times \frac{\Delta t}{2\Delta x}$$

Momentum conservation equation:

$$\frac{Du}{Dt} + g \frac{\partial h}{\partial x} = 0$$

$$\Leftrightarrow \frac{u_i^{n+1} - u_i^n}{\Delta t} + g \frac{h_{i+1}^n - h_{i-1}^n}{2\Delta x}$$

$$\Leftrightarrow u_i^{n+1} = u_i^n - g \frac{\Delta t}{2\Delta x} \times (h_{i+1}^n - h_{i-1}^n)$$

### 3.2.3 Boundaries conditions

#### Left boundary condition

The Left boundary condition is set as constant flux boundary of water. It represents a local punctual groundwater flood influx.

#### Right boundary condition

The right boundary  $x_N$  is constrained by the length location of the last point. Flux at the end point is computed using velocity and height at this location.

#### Visualization

The results of the Saint-Venant numerical model in Lagrangian reference are illustrated Figure 3.4 and Figure 3.5 at time  $t = 10$  s,  $t = 70$  s. The space time step was  $dx = 50m$ , with  $N = 21$  nodes and  $dt = 0.01s$ .

## 3.3 Fully Lagrangian fluid dynamic description: The Verlet scheme

A fully Lagrangian description needs  $x(t, \phi)$  independent of  $dx$ , where  $\phi$  is the number of the particle. The Verlet scheme is adapted to this problem, it

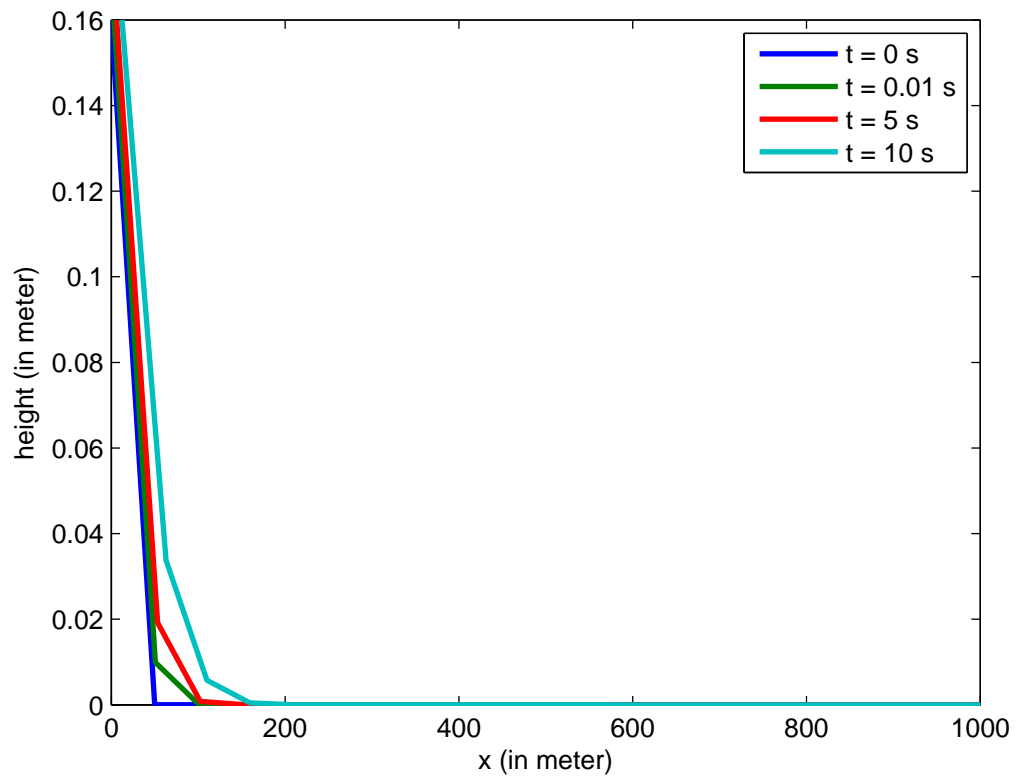


Figure 3.4: 1D Saint-Venant flow at  $t = 10$  s (Computation FORTRAN, visualization MATLAB)

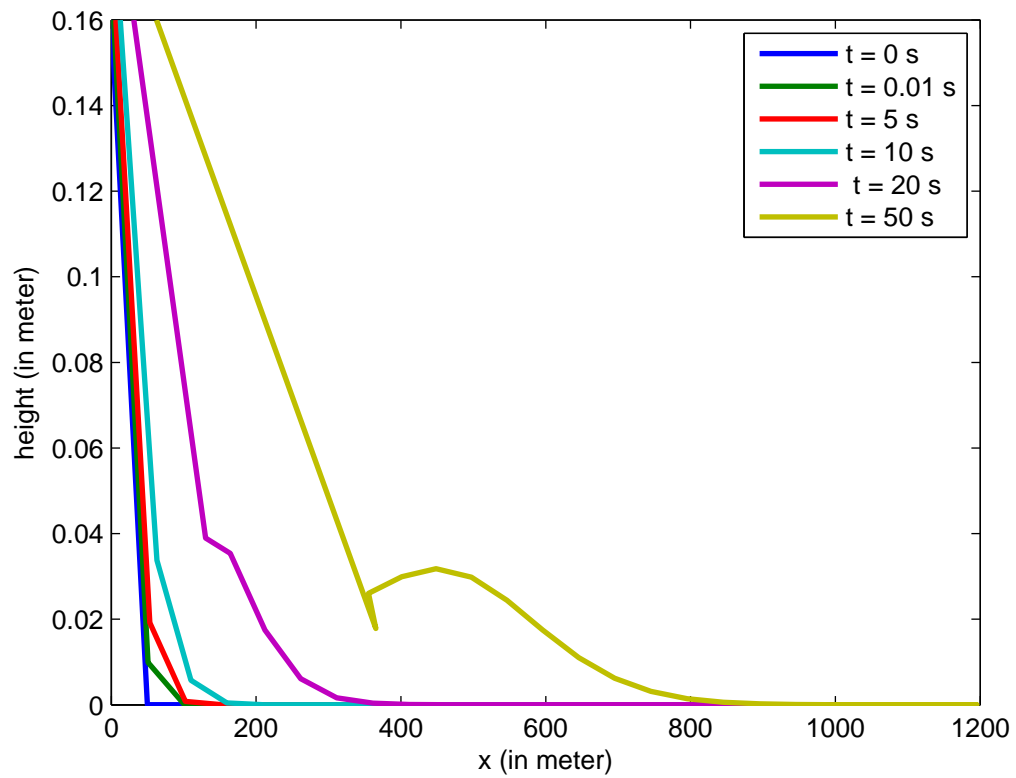


Figure 3.5: 1D Saint-Venant flow at  $t = 70$  s (Computation FORTRAN, visualization MATLAB)

develop a full Lagrangian description of the fluid particle.

### 3.3.1 Mathematical formulation

Using mass conservation, we define  $\Delta x$  by the equation,

$$h\Delta x = \Delta c$$

where  $\Delta c$  is considered as the mass of fluid, is constant in each cell  $\Delta x$  except at inflow.

## 3.4 Global and local mass conservation

The height at the initial condition is defined  $h_x(t) = 0.005 + (1 - x(y)^{1/2})^2$  the total mass is now not constant due to the flux from the SWE part (and from the possible non-zero diffusive flux from the Spreading part but let's ignore that). So, defining  $\theta(t)$  as the total mass take the rate of change  $\dot{\theta}$  to be the flux from the SWE. The main new feature is that the partial masses cannot remain constant in time since the total mass is not constant in time. However, the normalized partial masses can remain constant in time, that is

$$\left(\frac{1}{\theta(t)}\right) \int_a^x h dx = c = constant \quad (3.12)$$

When the time differentiation is carried out, an additional term  $c\dot{\theta}$  on the right hand side has to be used.

1. Momentum equation.  $x, u$ , the position and the velocity are advanced from

$$\frac{dx}{dt} = u, \quad \frac{du}{dt} = -\frac{g\Delta h}{\Delta x} = -\frac{gh\Delta h}{\Delta c}$$

2. Continuity equation. The height  $h$  is advanced from

$$h\Delta x = \Delta c$$

### 3.4.1 Discretization and algorithm implementation

We start from the momentum equation in a Lagrangian domain:

$$\frac{Du}{Dt} = -g \frac{h\Delta h}{\Delta x} \quad (3.13)$$

To compute the mesh location, we use the Velocity Verlet formulation (Dummer et al., 2012 [13]).

First step :

$$\frac{x_i^{n+\frac{1}{2}} - x_i^n}{\frac{\Delta t}{2}} = u_i^n \quad (3.14)$$

Second step :  $h^{n+\frac{1}{2}}$  is computed by the relation

$$h^{n+\frac{1}{2}} \Delta x^{n+\frac{1}{2}} = \Delta c \quad (3.15)$$

$$\frac{u_i^{n+1} - u_i^n}{\Delta t} = -\frac{gh^{n+\frac{1}{2}}\Delta h}{\Delta c} \quad (3.16)$$

$$u_i^{n+1} = u_i^n - \frac{gh^{n+\frac{1}{2}}\Delta h^{n+\frac{1}{2}}dt}{\Delta c} \quad (3.17)$$

Third step :

$$\frac{x_i^{n+1} - x_i^n}{\Delta t} = \frac{1}{2}(u_i^n + u_i^{n+1}) \quad (3.18)$$

### 3.4.2 Numerical Results of Saint-Venant equations using the Verlet scheme

#### Initial conditions

The initial conditions are not known for this equation because no exact solution is available for this problem. We tested three different height initial conditions for:

1.  $h^0 = a \times \left(1 - \left(\frac{x^2}{4}\right)^2\right)$  with  $a = 0.01, 1...10$  and  $x = [0, 2]$  The result obtained are illustrated Figure 3.6. The displacement of the water wave, its location and height is illustrated. After the first time step, the height of the water column at the left boundary drop to its real dynamic height maintained by the inflow.

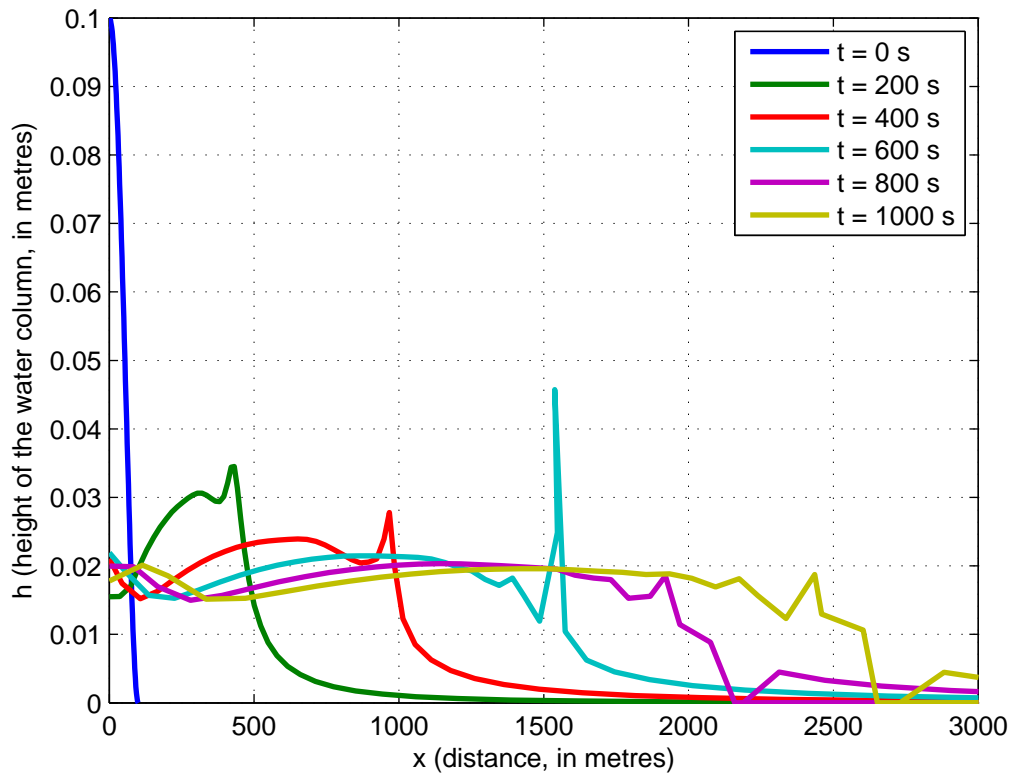


Figure 3.6: Results of the computation of the Saint-Venant equations using the Verlet scheme,  $N = 51$  nodes and initial condition  $h^0 = a \times \left(1 - \left(\frac{x^2}{4}\right)^2\right)$  (Computation and visualization tool MATLAB).

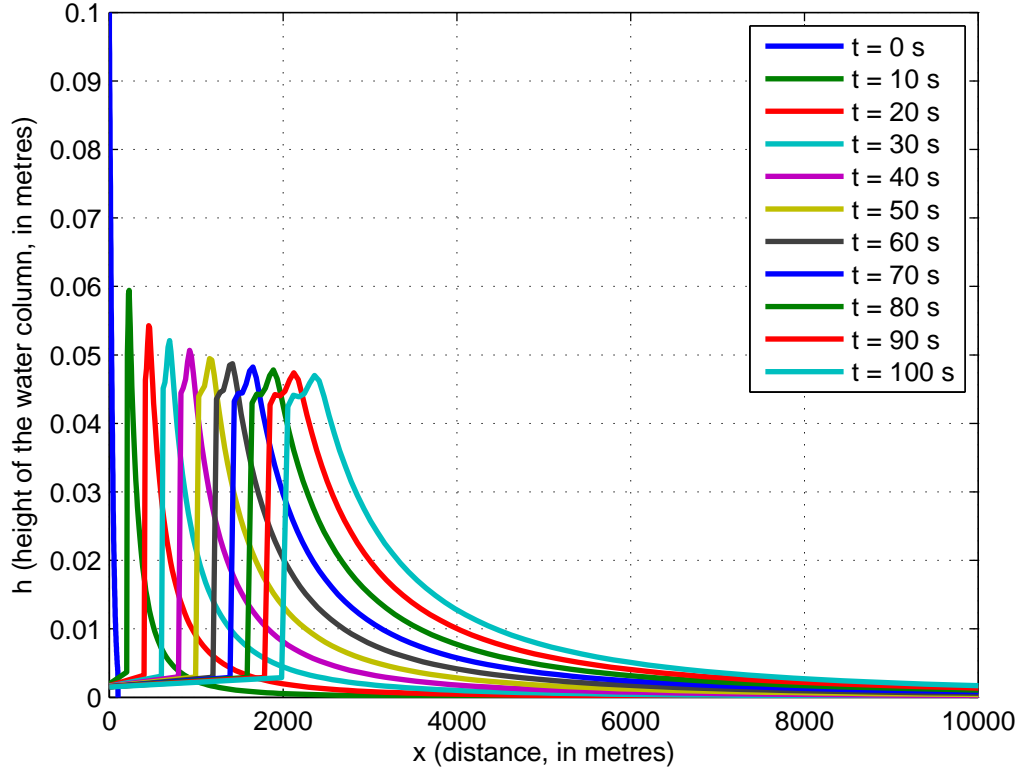


Figure 3.7: Results of the computation of the Saint-Venant equations using the Verlet scheme,  $N = 11$  nodes and initial condition  $h^0 = a \times (1 - \tanh(x))$  (Computation and visualization tool MATLAB).

2.  $h^0 = a \times (1 - \tanh(x))$  with  $a = 0.01, 1 \dots 10$  and  $x = [0, 2]$  The result of the computation of the Lagrange Saint-Venant equations using the Verlet scheme is illustrated Figure 3.7. It shows the evolution of the water height column over time.
3.  $h^0 = 1$  for  $x = [0, 50]$  and  $h^0 = \left(1 - \left(\frac{x^2}{4}\right)^2\right)$  for  $x = [50, 100]$ , ,  $dt = 0.00001s$ ,  $dx = 1m$ . The result of the computation of the Lagrange Saint-Venant equations formulation using the Verlet scheme is illustrated Figure 3.8 and zoom on the wave front illustrated Figure 3.9 and the left boundary Figure 3.10 and the oscillation on the front Fig-

ure 3.11. It shows the evolution of the water height column over time. Oscillation due to the sharp initial condition and the explicit method (Figure 3.11). The Figures 3.8 and 3.11 illustrates the instability of the scheme mainly due to the initial condition and highlight the difficulty the set up the correct initial condition. The inflow is fixed to  $q_{in} = 0.2m^3.s^{-1}$  and the initial water height column is set up to obtain a height that  $h_0 = 0.1m$  at  $t = 0s$

### Boundary condition

**Left boundary, velocity of nodal point 0** The left boundary is a Neumann boundary with a fix flux. It represents the inflow of water from the source. The position of the node 0 is  $x(t)_0 = 0$ .

**Right boundary, velocity of nodal point N** The right boundary is defined by the moving node boundary  $x_{N+1}$ , at that location the local mass is considered as  $c_N = 0$  and in theory, the height of the water column is  $h_N = 0$ . The velocity of the point is defined by the equation:

$$v_N^{n+1} = v_N^n \tag{3.19}$$

It is also possible to fix a value for  $h_N$  and  $dh_N$  while considering the value of  $h_{N+1}$  and  $dh_N$  as higher.

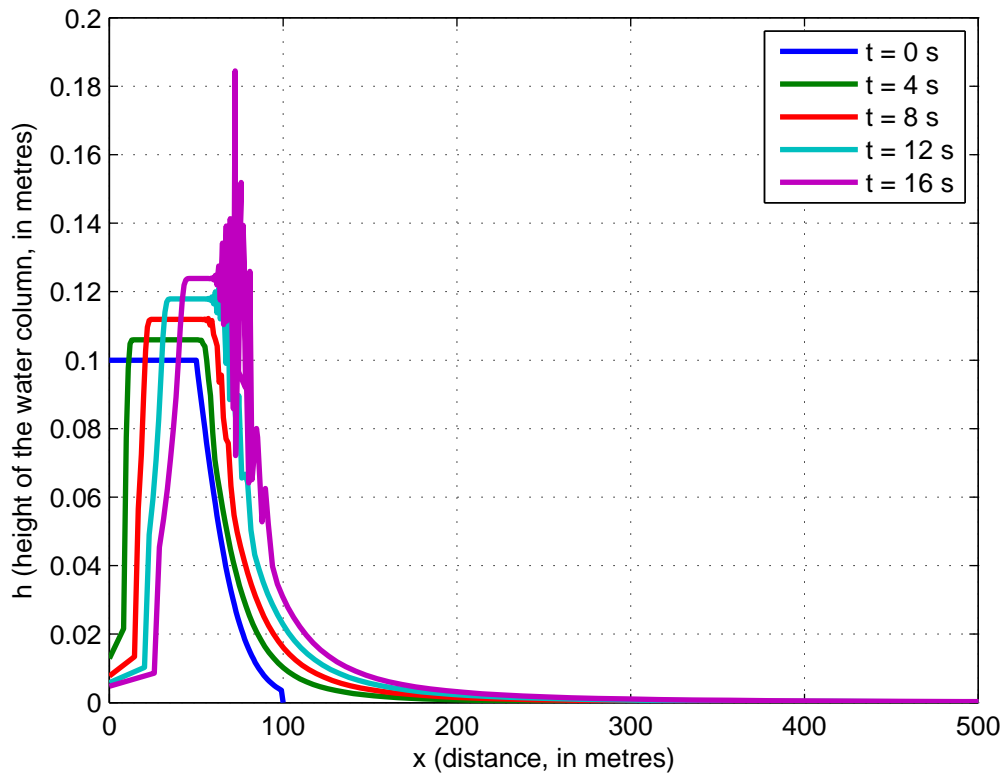


Figure 3.8: General results of the computation of the Saint-Venant equations using the Verlet scheme,  $N = 101$  nodes and initial condition  $h^0 = 1$  for  $x = [0, 50]$  and  $h^0 = \left(1 - \left(\frac{x^2}{4}\right)^2\right)$  for  $x = [50, 100]$ ,  $dt = 0.00001s$ ,  $dx = 1m$  (Computation and visualization tool MATLAB).

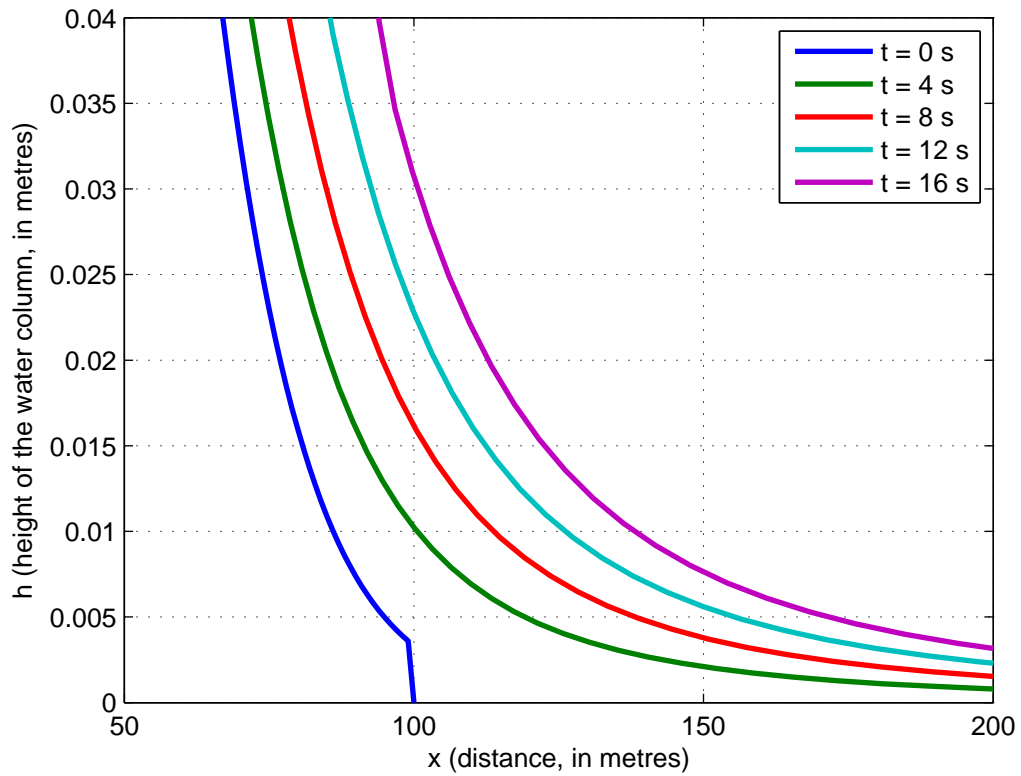


Figure 3.9: Front zoom results of the Saint-Venant equations computation using the Verlet scheme,  $N = 101$  nodes and initial condition  $h^0 = 1$  for  $x = [0, 50]$  and  $h^0 = \left(1 - \left(\frac{x^2}{4}\right)^2\right)$  for  $x = [50, 100]$ ,  $dt = 0.00001s$ ,  $dx = 1m$ . Zoom on the front wave (Computation and visualization tool MATLAB).

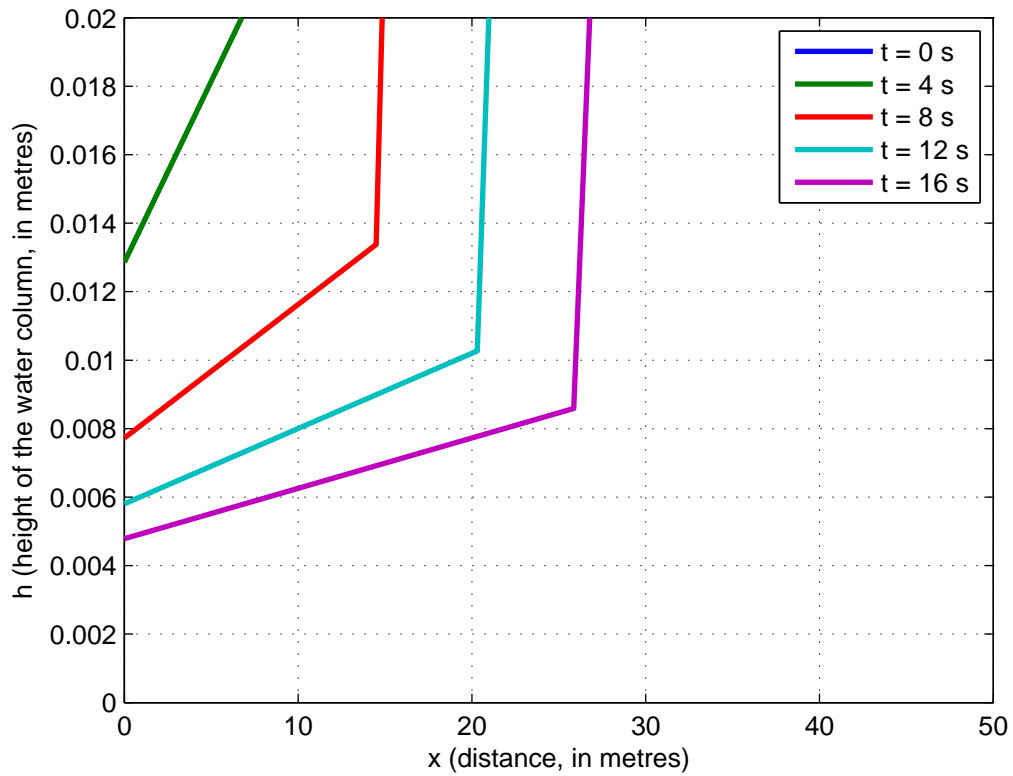


Figure 3.10: Left boundary results of the Saint-Venant equations computation using the Verlet scheme,  $N = 101$  nodes and initial condition  $h^0 = 1$  for  $x = [0, 50]$  and  $h^0 = \left(1 - \left(\frac{x^2}{4}\right)^2\right)$  for  $x = [50, 100]$ ,  $dt = 0.00001s$ ,  $dx = 1m$ . Zoom on the Left boundary (Computation and visualization tool MATLAB).

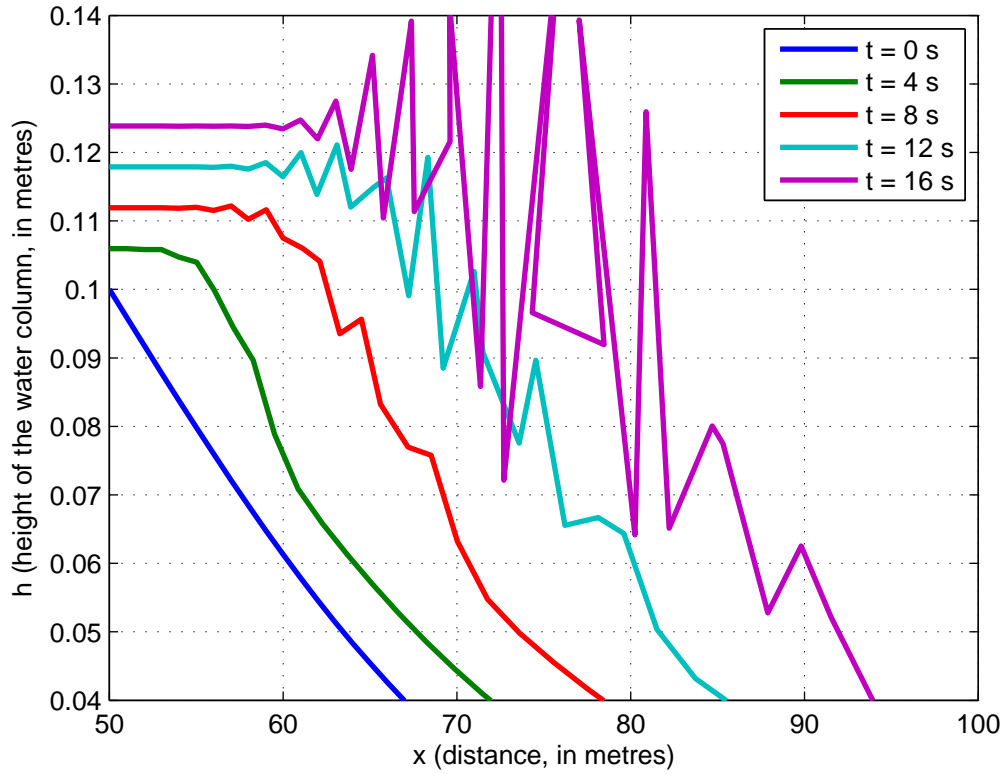


Figure 3.11: Oscillations on the water front associated with the Saint-Venant equations computation using the Verlet scheme,  $N = 101$  nodes and initial condition  $h^0 = 1$  for  $x = [0, 50]$  and  $h^0 = \left(1 - \left(\frac{x^2}{4}\right)^2\right)$  for  $x = [50, 100]$ ,  $dt = 0.00001s$ ,  $dx = 1m$ . Zoom on the Left boundary (Computation and visualization tool MATLAB).

# Chapter 4

## Non linear diffusion: Thin film equation

The thin film equation, a non linear diffusion equation, also called the lubrication approximation, is used to model the front wave of the groundwater flood. The thin film equation is a 4th order in space 1st order in time, partial differential equation. It is used to compute the height versus spreading of a thin film of liquid on a surface over time. The equation is defined as :

$$\frac{\partial h}{\partial t} = \frac{\partial}{\partial x} \left( h^n \frac{\partial h}{\partial x} \right) \quad (4.1)$$

where  $n = 3$ . The solution of the self similar problem when  $n = 1$  has been study before with Finite Element (Bhattacharya, MSc 2004 [8]) and Finite Difference (Baines et al., 2011 [7]) and Bird, 2012 [14]). The analytical solution for the case of  $n = 3$  haven't been discovered yet, no initial condition can be surely used for that case.

### 4.1 Mathematical formulation

The algorithm to model the thin film equation is again based on local mass conservation.

1. Advance  $x$  the position of the film and  $h$  the height of the water using

$$\frac{dx}{dt} = h^3 h_{xxx}$$

2. Advance  $h$  using local mass conservation

$$h\Delta x = \Delta c$$

We use the interface boundary conditions: continuity of  $h, u, h_x$  and the free boundary conditions:  $h = h_x = h^3 h_{xxx} = 0$ . Also, the inflow boundary conditions at the interface:

$$\frac{d}{dt} \int h dx = \frac{d}{dt} (h\Delta x) = \text{given flux}$$

## 4.2 Finite Difference discretization

There is no analytical solution to this partial differential equation. In order to test the numerical, the initial condition is fixed arbitrarily to:

$$u^0 = (1 - x^2)^2 \quad (4.2)$$

The initial mesh is regularly spaced but later deformation will occur resulting in non uniform mesh. A condition on the time step has to be strict to avoid node overtaking. Nodes are not allowed to cross each other since the conservation principle breaks down. We write

$$\frac{dx}{dt} = u, \quad u = h^3 h_{xxx}$$

We pose that

$$q = -h_{xx}$$

giving

$$u = -h^3 q_x$$

To approximate  $q$ , we use:

$$u_i = -(q_i)_x \approx -\frac{\frac{(h_{i+1}-h_i)}{(x_{i+1}-x_i)^2} + \frac{(h_i-h_{i-1})}{(x_i-x_{i-1})^2}}{\frac{1}{x_{i+1}-x_i} + \frac{1}{x_i-x_{i-1}}} \quad (4.3)$$

We obtained an approximation of  $q_i$  for each nodal points and can compute the velocity value by using 4.3. From this result, the location of the nodal

points  $x_2$  until  $x_N$  can be determined using an explicit Euler method. We used forward Euler to compute the new nodes location

$$x_i^{n+1} = x_i^n + u^n dt$$

The height is determined using the local mass. From the initial condition using central differences, we have

$$\rho_i = (x_{i+1}^0 - x_{i-1}^0)h_i^0$$

for  $i = 2, \dots, N - 1$  Here,  $x^0$  is a vector containing the initial mesh location and  $h^0$  is the vector containing the initial water column height.

## 4.3 Boundary conditions

### 4.3.1 Left boundary, velocity of nodal point 0

The left boundary is a flux boundary. A amount of water filled the first grid block at each time step. The mass of the local block  $c_0$  is defined as:

$$c_0(t + 1) = c_0(t) + dt \times q(t) \quad (4.4)$$

In our case, a constant flux is used for simplification and  $q(t) = 1m^3.s^{-1}$ . The left boundary is computed using symmetry principle or mirror point along the  $y$  axis defined by the equation:

$$h_0^n = \frac{c_0^n}{2 \times x_0^n} \quad (4.5)$$

with  $c_0 = cst$  computed at the time  $t = 0$  at initial condition.

### 4.3.2 Right boundary, velocity of nodal point N: Thin film precursor

The right boundary is defined by the moving node boundary  $x_{N+1}$ , at that location the local mass is considered as  $c_N = 0$  and in theory, the height of the water column is  $h_N = 0$ . Considering that height and the fact that  $h$  is used to compute the velocity of the node, velocity will be 0. A thin

film precursor has to be used. A thin film precursor has to be added to the numerical model. O'Brien [6] described the precursor thin film as a thin layer to allow the liquid to move. On a numerical point of view, the thin film precursor is computed through the height given at the node  $x_N(t)$ . If  $h_N(t) = 0$ , we have  $v_N(t) = 0$  and the node  $N$  doesn't move as illustrated by the equation 4.6:

$$v_N(t) = -h_N(t)^2 \times \frac{(q_N(t) - q_{N-1}(t))}{(x_N(t) - x_{N-1}(t))} \quad (4.6)$$

## 4.4 Numerical Results of the thin film equation

The Figure 4.1 illustrates a half domain time stepping method evolution of the thin film equation including a precursor film at the front of  $h_N(t) = 0.05m$ . The line shows the shape of a droplet spreading over a surface at time  $t = [0s, 2s, 4s, 6s, 8s, 10s, 12s, 14s, 16s, 18s, 20s]$ . The time step  $dt = 0.000001s$  for a space step of  $dx = 0.2m$  over 2 metres long. The high of the water column is fix at a maximum of  $h_0(0) = 0.1m$ . To optimize the computation velocity, the number of nodes have been chosen to  $N = 11$  including a fix node at  $x_0(t) = 0$  and a free boundary at the node  $x_N(t)$ . For higher time or space step, the solution blows up. The result shows the free moving boundary node moving on the right as expected by previous author publication. The curvature of the droplet contact between water and air is getting flatter as expected to assure mass conservation. The left boundary present trend  $\frac{dh}{dx} = 0$ . The dynamic angle as illustrated by O'Brien [6] decreases. The Figure 4.2 resumes the main features of the half thin film equation problem.

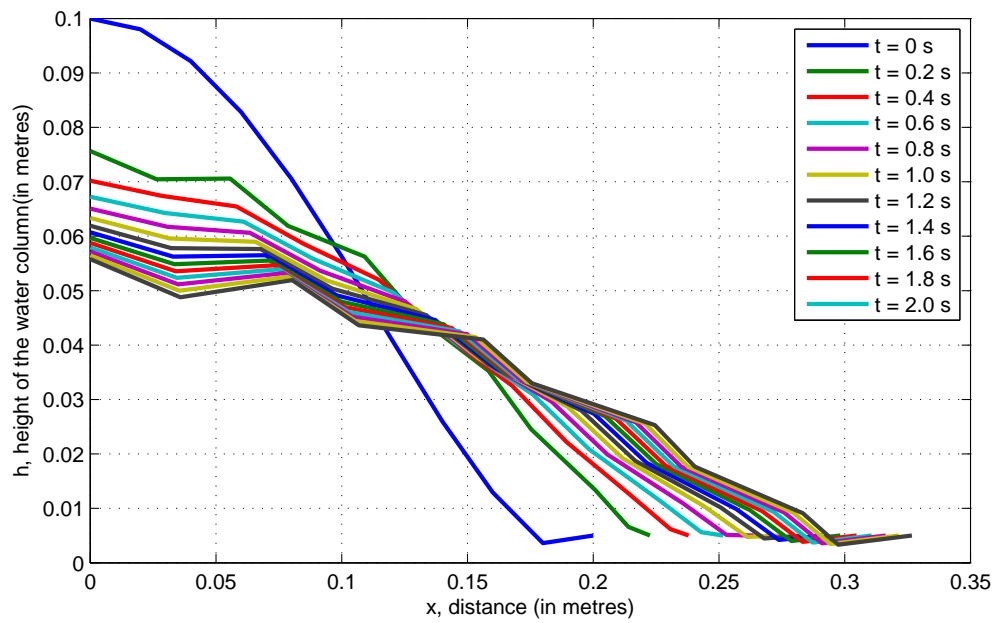


Figure 4.1: Results of the computation of the thin film equation for  $N = 11$  nodes.(Computation and visualization tool MATLAB)

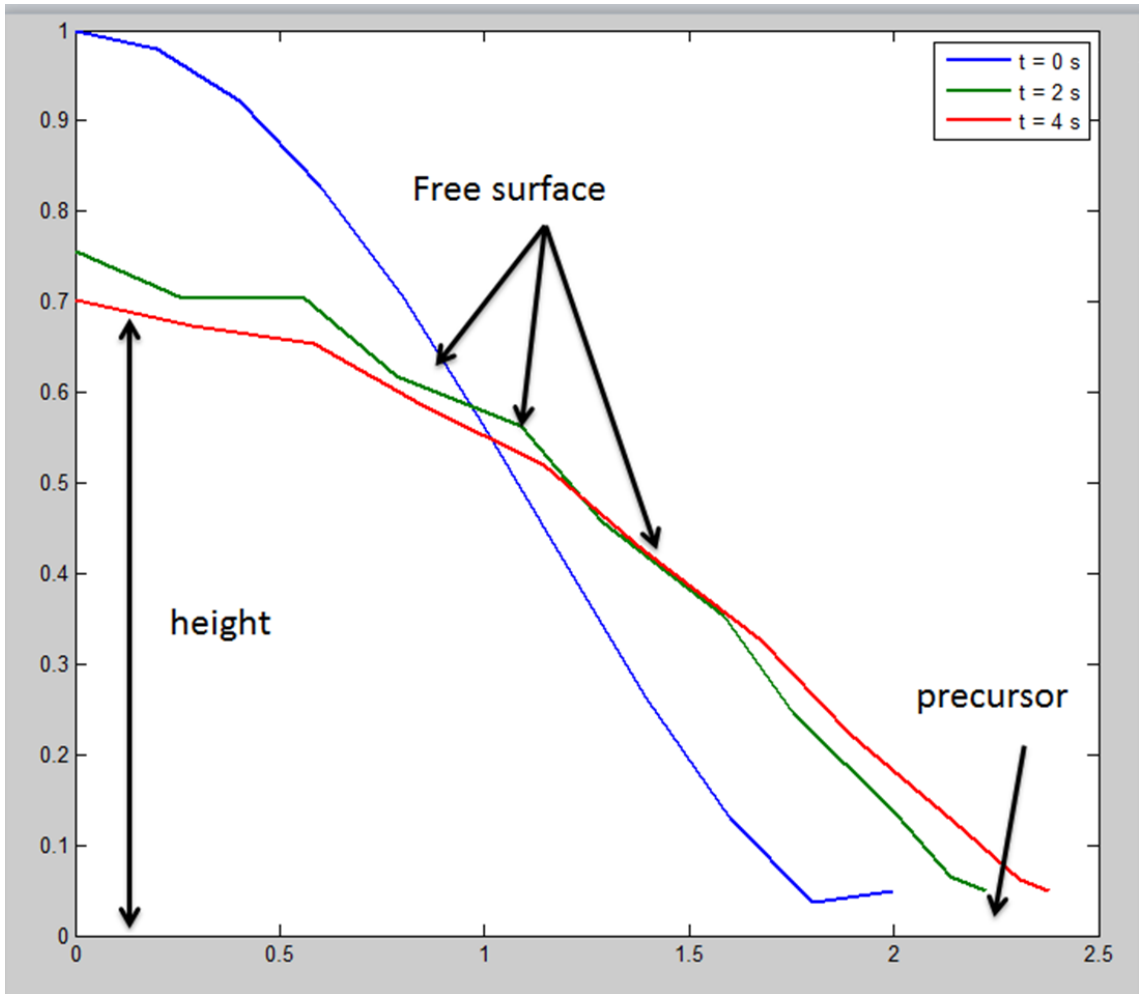


Figure 4.2: Illustration of the main features of the thin film script (Computation and visualization tool MATLAB).

# Chapter 5

## Coupling model for flood modelling

The coupling of the two numerical schemes needs careful examination of both flow domains. Time step are different and the interfaces point has to be identified. At the interface of the two flows domains, there is continuity of the water column height, velocity of the fluid, the water flow, slope of the continuity of the water column height.

We introduce  $x_I$ , the left boundary point which is at a constant location  $x_I = 0$ .  $x_C(t)$ , the moving boundary point between the two domains and  $x_F(t)$ , the right boundary point at the front of the water wave. The moving mesh strategy is used for both domains through the Lagrangian frames of reference used. The Figure 5.1 resumes and illustrates the numerical problem with the main features associated. We have a 4th order equation; we need 4 boundaries conditions with 2 moving boundaries, we need also 2 more boundary conditions.

### 5.1 Mathematical formulation

We define the condtion at the node 0,  $C$  and  $N$ . At  $x_C(t)$ , we have:

$$v_{SW} = v_{TF}$$

$$h_{SW} = h_{TF}$$

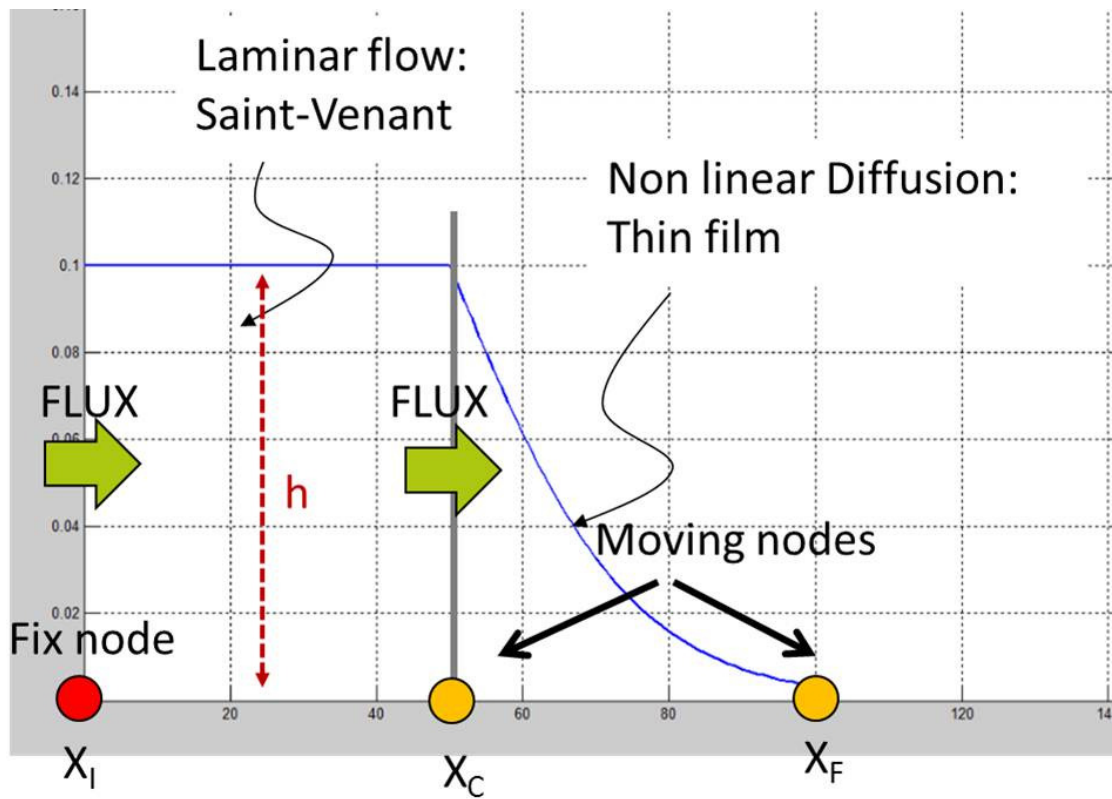


Figure 5.1: Schematic illustration of the coupled flow problem

and

$$\frac{\partial h}{\partial x}\Big|_{SW} = \frac{\partial h}{\partial x}\Big|_{TF}$$

The boundary conditions at

$$x_F(t)$$

are

$$\begin{aligned} h_{TF} &= 0 \\ \frac{\partial h}{\partial x}\Big|_{TF} &= 0 \end{aligned}$$

The condition  $h_N = 0$  gives a zero flux condition on the right boundary.

## 5.2 Global and local mass conservation

In order to model the flux of water at the interface of the two domains at the location of the moving node, a transfer flux function has to be implemented. We use a partial mass coefficient to assure a smooth redistribution of the water over the whole domain by normalization. The coefficient  $\theta$  is defined as

$$\theta_i(t) = \int_a^x h_i dx = c_i \quad (5.1)$$

The global mass conservation equation became:

$$\int_a^x h(t) + [hv]_a^x = \dot{c} \quad (5.2)$$

With:

$$\theta^{new} = \theta^{old} + dt \times \dot{c} \quad (5.3)$$

And each local mass:

$$h_i \times (x_{i+1} - x_{i-1}) = c_i \theta^{new} \quad (5.4)$$

The moving mesh method for the Verlet scheme was coupled with the moving mesh of the thin film equation in away that the mesh doesn't overlap. First results were obtained for the model. Conservation principle of the water mass applies by local conservation mass. A normalization principle was used as described previous to distribute the inflow mass increase from the left boundary over the whole domain. Nevertheless the result exhibit flow continuity problem over the domain at the common node.

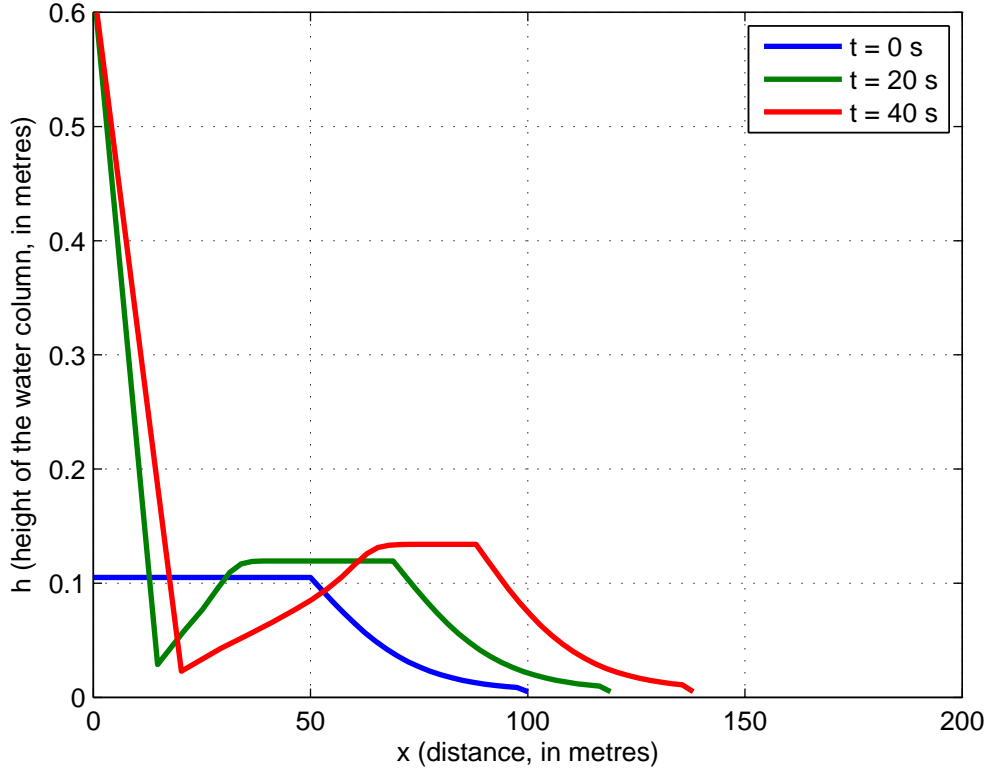


Figure 5.2: Numerical result of the coupled model at time  $t = 0$  s,  $t = 20$  s and  $t = 40$  s

### 5.3 Numerical modelling results

Result obtained by the coupled model is illustrated Figure 5.2 and Figure 5.3. The two domains of flow are visualized on the model as well as there evolution over time. The number of node was fixed to  $N = 41$ , the time step to  $dt = 0.00005s$  and the space discretization to  $dx = 2.5m$ . The solution shows a problem of continuity of the left border due to the flow boundary and the change of the high due to the change of velocity. Another issue came at the point  $x_C$  where the continuity seems to be assured. Oscillation on the left border arises after  $t = 200s$  and cause a solution blow up later. The solution proposes is on it draft level and will need further testing and improvement to propose a better solution even if the moving mesh of the two

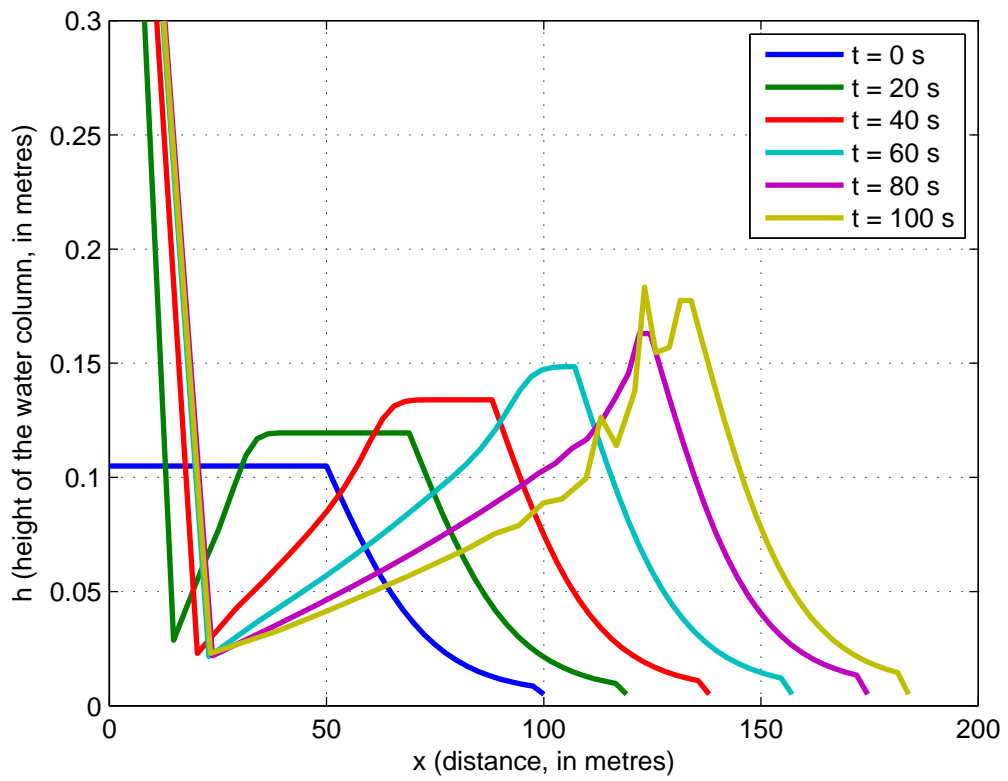


Figure 5.3: Numerical result of the coupled model at time  $t = 0$  s,  $t = 20$  s,  $t = 40$  s,  $t = 60$  s,  $t = 80$  s,  $t = 100$  s

flow domain is assured.

# Chapter 6

## Conclusions and Further Work

### 6.1 Conclusions

During this project, the Saint-Venant and thin film equations have been used. Several schemes were tested to optimize the resolution of the Partial Differential Equations. To solve the Saint-Venant set of equations, explicit Eulerian and Lagrangian methods were used. The central space difference was used for the Eulerian method, the scheme show some instability at it left boundary. Furthermore, a volume corrector is used to recalculate the height of the wave at the location of the node based on flux difference between the next and the previous node. Semi-Lagrangian and fully Lagrangian method were used as well. The semi-Lagrangian offers an intermediate method more accurate than the Eulerian with the simple formulation of a transformed Euler formulation. The fully Lagrangian formulation was solve using the "Verlet method" based on two half location time step computation with a height computation between the two half time step. It offers a strong stability of the scheme. The "Verlet method" is a moving mesh method; the method we used is a velocity based method. The importance of Lagrangian method is highlighted by the results. Nevertheless, the initial condition plays a strong role in the scheme stability. Even if Saint-Venant equations have analytical solution in certain situation, it doesn't apply to all configurations. We designed the initial condition based on supposition like a  $1 - \tanh(x)$  function. Eulerian methods are very popular because of it visualization. Lagrangian methods are more accurate but need some practice to be familiar with. The left boundary considered as a flux boundary represents the inflow of the flood

in the model. The amount of flux was fixed based on the volume of water already set by the initial condition. The flux boundary was handled by two methods, the filling of the first node by the flux and a distribution of the flux over the whole water domain using partial local mass coefficient.

The thin film equation using dynamic mesh introduces to interesting applied numerical modelling problem, its resolution is a well known problem. Method, time step and mesh discretization size as well as initial condition have strong consequence on the stability of the solution and the rise of oscillations.

Due to the high instability of some methods, some schemes have to be preferred or corrector applied like the volume corrector for the central space difference method or FTCS method (Forward Time Central Space). Nevertheless, the results obtained are similar to current publication in terms of expected results. Some problem arises at the left flow boundary due to the calculation of the water high based on local mass conservation issue.

The result obtained for the coupled model needs further work to improve the model and constitute only a promising draft test to model groundwater flood in a more accurate manner than actual model.

The use of a thin film to describe a flood could be seen as "strange". But coupled with Saint-Venant set of equations and for low water level between 0 and 0.1 metres, it could improve the description of the front wave in a more accurate manner for groundwater flood event.

The slope of the area was not considered as well as the roughness of the area. Those parameters will increase or decrease the velocity, the travel time and the height of the water wave. Measuring the roughness of area based on satellite image is a research subject.

## 6.2 Results

Results obtained during this thesis project gives direction to the development of improved flood model based on coupled physical flow model. The first draft coupled model is under development and the result constitutes only a first draft result. Limitation of the method and gap in the flow continuity are

evident. The use of coupled flow domain approach to model a groundwater flow is original for multidisciplinary research purpose on hydraulic, groundwater model and advance numerical modeling. The ideas developed during this thesis will need further validation, implementation and development.

## 6.3 Further Work

Several direction have to be considered for further work:

1. A first improvement will be to develop the model with implicit method which offers better result in term of scheme stability and accuracy. Nevertheless, computation time will be considerably increased. In the case of the thin film equation which need small time step the computation time could became a problem.
2. A second direction will concerned the two dimensional (2D) version of the models which will have an interesting ouput on the visualization of the wave.
3. A third direction will concerned the development of a complex topography solving method which take in count the altitude change of the area.
4. A last direction will concern the source point spread origin of groundwater flood source: Our simple 1D model only considered a single water source. In a groundwater flood event, it is most likely that several flooding initial point will occurs at the same time according to their altitude. The flood wave will interact with each others. This complex mechanism will have to be modeled.

# Bibliography

- [1] Olsen, N.R., 2012. Numerical Modelling and Hydraulics, Department of Hydraulic and Environmental Engineering. NTNU. 3rd edition, 9.March 2012. ISBN 82-7598-074-7.
- [2] Delis, A. I., Kampanis N. A., 2010. Numerical flood simulation using depth averaged free surface flow models. The Encyclopedia of Life Support Systems, Theme 4.20 Environmental Systems, Topic 4.20.5 Computational Sustainability Analysis, Entry 2, Developed under the Auspices of the UNESCO, Eolss Publishers Co Ltd.
- [3] Dawson, C. and Mirabito, C.M., 2008. The shallow water equation. Lecture slides from the Institute for Computational Engineering and Sciences, University of Texas at Austin, USA.
- [4] OPEN OpenCFD currently distribute. Open FOAM. <http://www.openfoam.org/download/>, accessed May 30, 2012.
- [5] Floodplain Underground SENSors(FUSE). FUSE stands for Floodplain Underground SENSors- A high-density, wireless, underground Sensor Network to quantify floodplain hydro-ecological interactions. Consulted the 30 July 2012 <http://fuseproject.org.uk/>.
- [6] O'Brien, S.B.G. and Schwartz, L.W., 2002. Theory and modeling of thin film flows. Encyclopedia of Surface and Colloid Science, p.5283-5297.
- [7] Baines. M.J., Hubbardo. M.E., and Jimacko, P.K., 2011, Velocity-Based Moving Mesh Methods for Nonlinear Partial Differential Equations (with M E Hubbard and P K Jimack), Commun. Comput. Phys., Vol. 10, No. 3, pp. 509-576.

- [8] Bhattacharya. B., 2004 A moving finite element method for high order nonlinear diffusion problems.
- [9] Budd, C.J., Huang, W., Russell, R.D., 2009. Adaptivity with moving grids. *Acta Numerica* (2009), Cambridge University Press, 2009 pp. 1131.
- [10] Weller, H., Ringler, T., Piggott, M. and Wood, N., 2009 CHALLENGES FACING ADAPTIVE MESH MODELING OF THE ATMOSPHERE AND OCEAN, Meeting summary January 2010, American Meteorological Society p. 105-109.
- [11] Baines, M., Hubbard, M. E. and Jimack, P.K., A Moving Mesh Finite Element Algorithm for the Adaptive Solution of Time-Dependent Partial Differential Equations with Moving Boundaries (with ), *Applied Numerical Mathematics*, 54, 450-469 (2005).
- [12] Price, J.F., 2006, *Lagrangian and Eulerian Representations of Fluid Flow: Kinematics and the Equations of Motion*, Woods Hole Oceanographic Institution, Woods Hole, MA, 02543 <http://www.whoi.edu/science/PO/people/jprice> June 7, 2006. Consulted the 24th July 2012.
- [13] Dummer, J., A Simple Time-Corrected Verlet Integration Method, accessed June 8, 2012. <http://lonesock.net/article/verlet.html>.
- [14] Bird, N., 2012 A Finite Difference Scheme for Solving the Fourth Order Problem, June 1, 2012. University of Reading 9 pp. Unpublished.